Misalignments characterization for micro-CPV modules

Cite as: AIP Conference Proceedings **2298**, 050004 (2020); https://doi.org/10.1063/5.0032292
Published Online: 09 November 2020

Luis San José, Guido Vallerotto, Rebeca Herrero, et al.

Misalignments Characterization for Micro-CPV Modules

Luis San José[1, a)], Guido Vallerotto[1], Rebeca Herrero[1] and Ignacio Antón[1]

[1] *Institute of Solar Energy, Universidad Politécnica de Madrid, Avda/Complutense 30, 28040, Madrid, Spain*

[a)] Corresponding author: luisjavier.sanjose@upm.es

Abstract. A validated method for misalignments characterization through image acquisition has been adapted for measuring misalignments in micro-CPV modules with integrated tracking. Due to the tight mechanical tolerances and tiny optical elements in this type of technology, a robust image processing that reduces the detection uncertainty of the optical components position in the image is required in order to obtain a valid measurement. An image processing based on pattern recognition is presented with promising results in the accuracy of the detection.

INTRODUCTION

Although Concentrator Photovoltaics (CPV) has achieved important milestones in efficiency, prices are still considerably high compared to conventional flat-panel photovoltaics based on silicon solar cells. Regarding cost reduction as a competitive key factor, unconventional architectures are in vogue due to their potential to achieve this goal. One of these approaches, the micro-CPV [1], aims to micro-scale CPV systems. A cells' size reduction has some advantages while rises new challenges. On the one hand, reducing the bulkiness of CPV modules by its miniaturization offers an interesting potential in cost reduction and material saving in module assembly. Moreover, the module thickness reduction increases the module front side contribution to heat dissipation, making unnecessary the use of heat sinks or expensive thermally-resistant substrates. On the other hand, smaller sizes imply difficulties on the cells manipulation and interconnection and in reaching a proper alignment between the micro-optical system stages.

The reduced size allows implementing novel architectures as the integrated tracking [2], consisting on a system scheme where the module is fix and the POE or the cells plane displaces compensating the variation of the sunlight angle of incidence over the module aperture. This would avoid the expenses of a tracker system where CPV modules are mounted, but, instead, high angular tolerance lenses would be needed, as well as an internal mechanical system for maintaining the light-spot on the cells along the sun path. This architecture will not be viable on conventional CPV because of the thicker high-acceptance lenses required (which will increase the module cost and weight) and also because of the module dimensions increment that would require the integrated tracking. Micro-CPV modules with integrated tracking are of special interest in scenarios where high energetic density is required and result attractive to be used in rooftops [3] maintaining the versatility of conventional PV but with the efficiency of CPV systems.

Despite the high angular tolerances reached with novel concepts of lenses and Secondary Optical Elements (SOE), the mechanical assembly tolerances in architectures with integrated tracking are very tight [4], due to the pursued aim of tracking the sun with the minimum movement of the module elements. For example, micrometric errors in the position of the receivers (*i.e.*, solar cell plus SOE) with respect to the optics have an impact in the angular performance that may affect the module efficiency. Errors in the manufacturing process, such as the lenses array assembly, the cells attachment to the back plane, a lack of coplanarity between the receivers and the optics planes, or the tracking system mechanical tolerances may also affect the module performance. All these errors may imply misalignments between elementary units (a single cell with its corresponding optics), meaning that they do not share the same optical pointing vector. Characterizing the existing misalignments in a micro-CPV module gives a valuable information not only about the manufacturing process, but also about the performance of the integrated tracking system. Furthermore, it will help to understand the efficiency limitations in micro-CPV modules, locating its causes.

16th International Conference on Concentrator Photovoltaic Systems (CPV-16)
AIP Conf. Proc. 2298, 050004-1–050004-6; https://doi.org/10.1063/5.0032292
Published by AIP Publishing. 978-0-7354-4032-6/$30.00

In this work, a validated method based on image processing for misalignments characterization in CPV [5] is proposed to be applied to a novel micro-CPV module with integrated tracking. The indispensable considerations and the needed processing for successfully applying the method in micro-CPV technology are established and explained.

CONSIDERATIONS ON THE METHOD APPLIED TO MICRO-CPV

A method for misalignments characterization in CPV through image acquisition has been applied and validated in previous works [5], measuring known introduced misalignments with a maximum value of 0.45º±0.06º. The method relies on examining the receiver position with respect to its POE. The displacement of the receiver position with respect to its ideal optimal position (when the center of the receiver and the center of the lens coincide) is proportional and translatable into degrees, by mean of geometrical considerations, which represents the unit misalignment (Fig.1.a).

For analyzing the receiver position shift, a camera is used to acquire images of the receiver magnified through the lens. Later, the lens and the receiver positions are identified through image processing and the measured difference between them is translated into degrees. To characterize the misalignments of a whole module, information of all units is needed, thus, one image per elementary unit must be acquired. To compare several units, a common reference must be chosen, which is obtained if the camera is placed at the same position with respect to the unit under measurement.

In micro-CPV, the tiny dimensions and the tight mechanical tolerances require a very low measurement uncertainty, since micrometric misplacements of the receiver suppose misalignments of tenths of degrees. In this measurement, the main uncertainty sources are the camera positioning and the identification in the image of the lens and the receiver. On the one hand, the misalignments are defined with respect to a common reference, which must be equal among all the images. This absolute reference is the camera position with respect to the module, then, if the camera position varies with regard to the units measured, the lens and the receiver positions in the image are altered too, which will introduce an error in the measured misalignment. Therefore, the uncertainty due to the accuracy and repeatability of the camera moving system has to be lower than the lens-receiver positions difference intended to be measured (in the presented case study, an error in the camera position of 0.1mm introduces an error of 0.16º in the measured misalignment). On the other hand, the reduced size of micro-CPV components require high resolution images (*i.e.*, a high ratio of pixels per millimeter), reaching a good definition of both the receiver and the lens. If a sharp image of both is not achievable in a single acquisition, it is necessary to take two pictures (Fig.1.b) or to forward bias the module to emit light, and therefore to have the lens and receiver edges well defined to be detected.

CASE STUDY: MICRO-CPV MODULE WITH INTEGRATED TRACKING

A novel micro-CPV module with integrated tracking has been measured with the mentioned method. The module is composed by 1mm square triple junction solar cells with a 1mm radius semispherical glass SOE attached to them. The POE is formed by a 8.34mm side hexagonal biconvex lens molded in PMMA glued to a rigid glass substrate. Since the POE's field of view is high (~60º), an integrated tracking mechanism displaces the receivers' plane to track the light spot position, which moves in X, Y and Z direction as the light incident angle varies, with ±12mm maximum travel in the XY plane. The lenses array is composed by 576 POEs in honeycomb structure. The module has been fixed to the base of an automated two-axes moving platform composed by XY stages with ±5µm movement precisions where a 16 Megapixels (Mpx) Ximea CCD (Charged Coupled Device) camera with a KAI 16000 sensor is mounted (Fig.1.c). With this configuration, a 36-lens array has been measured as described previously (taking two pictures per unit: one focusing to the receiver and other to the lens). The camera has been aligned with a first reference lens, and as the exact lenses dimensions are known, it has been displaced predefined distances to the rest of lenses centers.

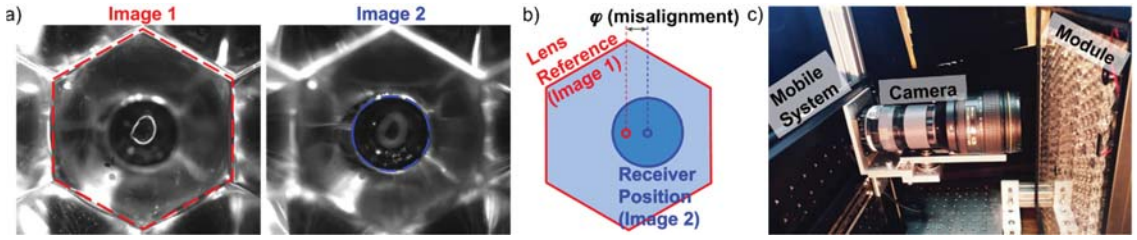

FIGURE 1. a) Lens and receiver image; their relative position is proportional to the misalignment (b). c) Used set up.

IMAGE PROCESSSING

A fundamental aspect of the method strikes in determining with low uncertainty the lens-receiver relative position, defined as the distance between the center of the receiver and the center of the lens. In the case study configuration, for example, an error of 7px (1% of the receiver size) in the determination of this distance implies an error of 0.1º in the misalignment determination, unacceptable for the aimed characterization (intended to measure misalignments as low as this value). An image processing for detecting univocally the receiver and the lens position with an uncertainty under 3px (~0.04º) at least is essential to obtain the absolute misalignment value. Thus, using the MATLAB image processing utilities and adjusting properly their intrinsic aspects, the segmentation algorithms permit extracting the receiver and the lens shape from the images. An image preprocessing, using different filters and contrast manipulations (enhancing the desired characteristics) may increase the robustness of the segmentation. Once the receiver and the lens areas are clearly identified on the image, object detection algorithms as the Hough transform for circles and the template matching respectively determine their positions accurately.

Image Preprocessing

First, a median filter followed by a sharpening removes the CCD sensor thermal noise in the image and increases the contrast along the edges where different gray levels meet [6]. Then, a contrast adjustment increases and splits the gray levels in the image. Second, two different filtering are applied: a local Laplacian filter (LLF) [7] and a local contrast manipulation. The LLF smooths changes in main areas' gray values without affecting the sharpness, helping the local contrast adjustment to enhance the gray levels differences leaving strong edges unchanged. Without the previous LLF, a local contrast manipulation would separate not only the tones foreground from the background, but also the object aimed to be discerned in different regions. Finally, an image levelling using a multithresholding through Otsu's method [8] discriminates image regions (Fig.2); brightening clearer regions, darkening obscurer regions and remaining intermediate gray regions unchanged proportionally to the threshold that discerns it.

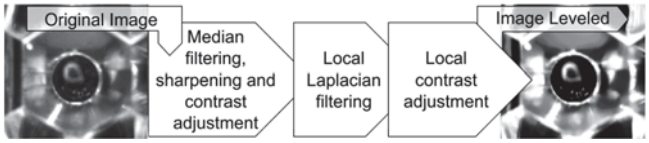

FIGURE 2. Image preprocessing for the receiver image.

Algorithms for Receiver Segmentation: Superpixel Oversegmentation (SPO) and Fast Marching Method (FMM)

To segment an image is understood as the process of dividing it into pixel sets (*i.e.*, objects) that are easier to analyze. In this regard, two different algorithms are used to define the receiver shape. The first, known as *superpixel oversegmentation* (SPO) [9], uses the simple linear iterative clustering (SLIC) for grouping the image pixels into k regions with similar values, using as weighting parameters the grayscale level and spatial proximity. The input of the algorithm is the number of desired regions (k). The initial seeds (starting points of the algorithm) are distributed on a regular grid over the image (Fig.3.b), which after the regions grouping, is converted into k regions on the image well adhered to the boundaries in the image (Fig.3.c). The image is then binarized using an Otsu multithresholding, separating univocally most of the receiver circular area from the background (Fig.3.d). Finally, some inaccurate segmented regions are refined by applying an opening on the image (a morphological operation that consists on an erosion followed by a dilation with the same structuring element [10]), that remains boundaries unaltered (Fig.3.e).

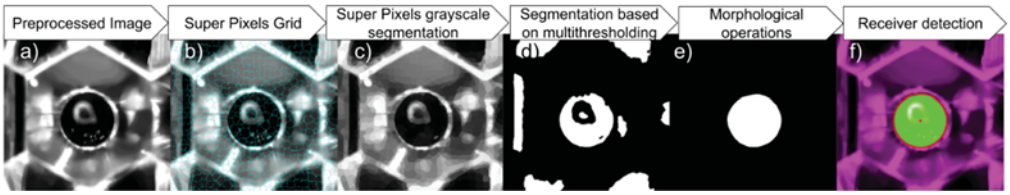

FIGURE 3. Super Pixels algorithm steps to segment the receiver area (e). Circle of (e) detected by the Hough transform (f).

The other segmentation algorithm is the *Fast Marching Method* (FMM) applied to image processing, consisting on the evolution of a predefined closed boundary as function of time in the normal direction, similar to a wave behavior. The contrast determines the evolution speed, lowering it when a strong contour is found (similar as when a wave encounters an obstacle), while the boundary shape evolution is determined each iteration by solving the Eikonal equation [11]. If the initial boundary (*i.e.*, the seed of the algorithm) is placed inside the receiver area on the image (Fig.4.a), the FMM finds the receiver boundaries in the preprocessed image with ease and accuracy (Fig.4.a-c).

Hough Transform for Circles

Both explained methods segment the round shape of the receiver (Fig.3.e and Fig.4.b). For estimating accurately the receiver position in the image, the Hough transform for circles is used [12] (Fig.3.f and Fig.4.c), whose inputs are the segmented receiver images and a range of radii values. The algorithm uses the pixels of the receiver region as candidates to vote in an accumulator, where each edge pixel is taken as a fixed radius circle center and casts votes in its circumference. A perfect circle would pile up its edge pixels' votes on a single accumulator position; thus, the position that hoards the greatest number of votes will be the receiver position. Because a range of radii is used for detecting the circular shape, one accumulator per radius value is created. Thus, for each image a circle with different center and radius value may be found. The output of the algorithm is an array comprising the detected circle center position, radius (inside the specified range) and probability metric (*i.e.*, the strength), which informs about the circle detection robustness and unicity. If the metric value is high, the probability of having a circle in the found position on the image is high; however, if there are several high values composing the metric array, many circles are likely to be found. The image preprocessing and the segmentation techniques used, may increase the metric value and make it unique, which is useful to determine which method detects better the receiver, and the needs of each algorithm.

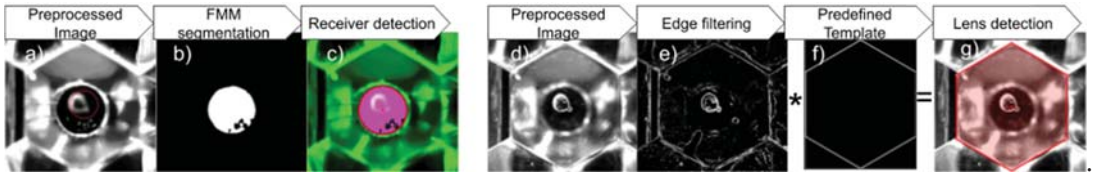

FIGURE 4. a-c) FMM for the receiver detection. d-e) Edge filtering and template matching are applied for the lens detection.

Image Processing to Detect Lenses

In the lens position determination, the same image preprocessing is applied (Fig.4.d). However, because the sharpness achieved by focusing the camera on the lenses plane, the hexagonal shape of the POE aperture is discerned using an edge filtering (Fig.4.e). As the lens size is known, a predefined template (Fig.4.f) with the hexagon dimensions may be used to find the lens position in the image through template matching (Fig.4.g). This algorithm drags the predefined shape along the image calculating the Normalized Cross Correlation (NCC) [13] in each point of the image where the template is placed. The point with the maximum NCC value is where the predefined shape best fits on the image (*i.e.*, the center of the lens) and thus, its values over the image inform about the detection robustness.

RESULTS

With the explained image processing and the measuring considerations commented, the lenses and receiver centers for 36 units have been detected to later assess their misalignments. When the FMM and the SPO are applied along with the preprocessing, both methods increase the metric with which the Hough transform determines the position of the receiver (circle). In Fig.5 an example of the Hough accumulators is shown for a particular image. The brightest point represents the point which is more probable to be the center of the receiver (related to the highest metric). On the right, the metric values of the different detected circles for these accumulators are represented in function of their distance (in pixels) from the stronger circle center (*i.e.*, the zero in the X axis). The higher is the metric of the detected center, the stronger its detection is. Moreover, the higher is the difference between the most probable circle metric and the second detected circle, the higher is its unicity, since it means that the second detected circle is much less probable to be the receiver shape than the first. It can be observed how the SPO has higher metric value and sharpens the metrics profile shape, indicating not only a more robust detected circle in this case, but also a unique position for its center.

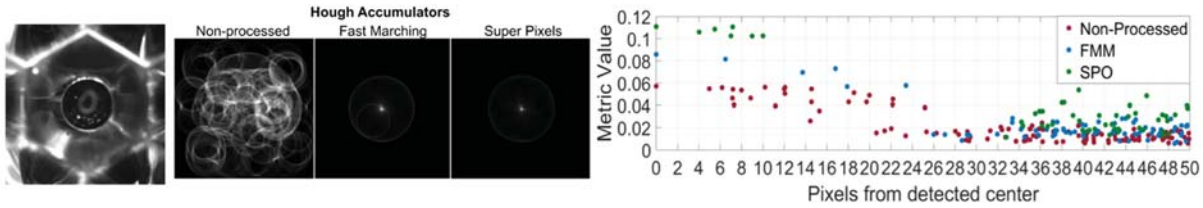

FIGURE 5. Hough transform accumulators for a particular image (on the left) obtained through the segmentation methods with image preprocessing and its metric distributions in function of the distance from the strongest circle center detected (right).

As in the previous graph, Fig.6 shows the metric distributions associated to the different detected circles (within a given radius range) for all the images without preprocessing (left) and applying them the preprocessing (right). The metric values are represented in function of the distance between centers, where X=0px corresponds to the most probable circle found. To robustly detect a circle, the metric distribution must have very high values for a single circle and low values for the rest of detected circles, which also must be far from the circle with maximum metric to not represent the receiver shape. In this regard, SPO reaches the highest metric values (blue to green points) and shows a good performance even without preprocessing. However, the FFM (red to yellow points) shows a poor performance without the preprocessing, but even applying it, it does not overcome the SPO metrics. The non-preprocessed FMM metrics are similar to the circle detection that results from the non-processed images.

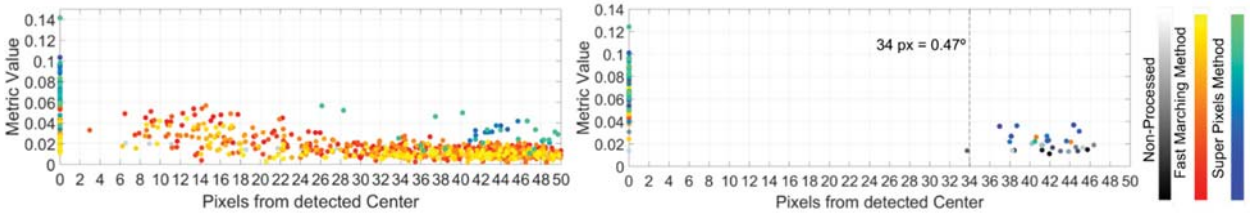

FIGURE 6. Metrics for images without (left) and with preprocessing (right) in function of the distance from strongest center.

For the lens position detection, a similar reasoning is followed. The parameter that in this case conditions the robustness of the detection is the NCC value. To explain this, in Fig.7 on the left, the accumulators of the NCC values obtained by template matching using two different thickness hexagonal templates are shown for a particular image. The brightest value in the accumulators corresponds to the most probable lens center location (*i.e.*, to the highest NCC value). On the center of the figure, the highest NCC values distributions corresponding to different detected hexagons for these accumulators are represented in function of their distance (px) from the most probable. To robustly detect the lens hexagon, the desired NCC distribution must include a high single value and a fast decrease to low values (while increasing distance from the most probable detected position).

The template used in the lens detection has to be enough edge-acquiescent to allow a strong detection in all the images, but also strict enough for determining a single lens center position. If the template edges are too thin (the case for 1px), there may be a poor fitting between the template and the image (thus, low NCC values). The detection may improve if thicker templates are used. However, if the template edges are too wide (*i.e.*, 10px in this case study), the positions where template fit are so many, that the NCC value keeps nearly constant for many detected lens positions.

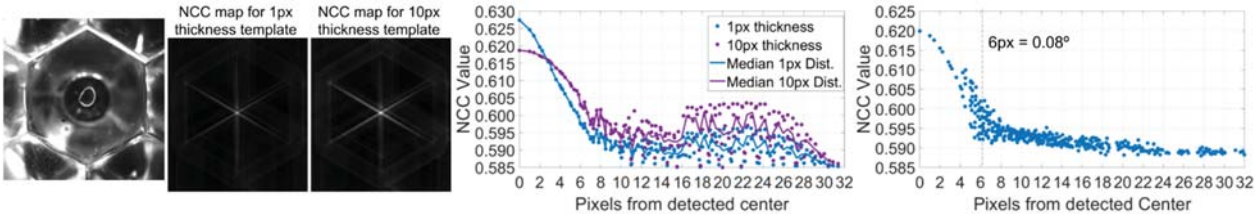

FIGURE 7. NCC accumulators for different thickness templates of an image (left). Highest NCC values distribution in function of the distance from the strongest detected lens position (center). Mean NCC values distribution for all the images (right).

The right side of the figure shows the mean NCC values distribution of the detected hexagons for all the images represented in function of the distance from the most robust hexagon detected (highest NCC value in each image)

using a 3px wide template (an edges width that showed the highest NCC values and a sharp transition to lower values than others). It can be noted that with high probability the lens center is identified in ±6px equivalent to ±54μm (±0.08º), an uncertainty that shows a good performance of the lens position detection through the proposed processing.

CONCLUSIONS & FUTURE WORK

The required conditions for applying a method based on image processing in micro-CPV misalignments characterization have been presented and established in this work. The developed image processing (that combines segmentation techniques with object detection algorithms) shows promising results in determining precisely both the lens and the receiver position in the images; however an uncertainty estimation of the method still has to be reached through different experiments. In the case of the receiver detection the superpixels oversegmentation yields better results in its area segmentation and does not require a preprocessing. In the case of the lens detection, the template matching shows a bounded uncertainty in the lens position determination, establishing a 3px edge-wide template as the optimum template edge width for the most robust detection. As future work, a complete and valid misalignments measurement in a micro-CPV module with its uncertainties and errors bounded will be aimed to be performed.

ACKNOWLEDGEMENTS

This work has been partially supported by FEDER / Ministerio de Ciencia, Innovación y Universidades – Agencia Estatal de investigación / Project MICRO-PV ref. ENE2017-87825-C2-1-R with cofounding from Comunidad de Madrid Program MADRID-PV2 P2018/EMT-4308,with co-funding from Fondo Europeo de Desarrollo Regional (FEDER) and Fondo Social Europeo (FSE) - Unión Europea. The authors also acknowledge the support of the European Commission through the H2020 project HIPERION (Grant Agreement 857775). This project has received funding from the European Union's Horizon 2020 research and innovation programme under Grant Agreement n°857775.

REFERENCES

1. C. Domínguez et al. "A review of the promises and challenges of micro-concentrator photovoltaics." AIP conference proceedings. Vol. 1881. No. 1. AIP Publishing LLC, 2017.
2. H. Apostoleris et al. "Tracking-integrated systems for concentrating photovoltaics." Nature Energy (2016): 1-8.
3. Liu, Xinbing, et al. "Design of Optical Elements for Low Profile CPV Panel with Sun Tracking for Rooftop Installation." 2017 IEEE 44th Photovoltaic Specialist Conference (PVSC). IEEE, 2017.
4. F. Duerr, et al. "Integrating tracking in concentrating photovoltaics using non-rotational symmetric laterally moving optics." Nonimaging Optics: Efficient Design for Illumination and Solar Concentration VIII. Vol. 8124. International Society for Optics and Photonics, 2011.
5. L. San José, G. Vallerotto, R. Herrero, and I. Antón, "Misalignments measurement of CPV optical components through image acquisition," Opt. Express 28, 15652-15662 (2020).
6. A. Polesel, G. Ramponi, and V.J. Mathews. "Image enhancement via adaptive unsharp masking." IEEE transactions on image processing 9.3 (2000): 505-510.
7. S. Paris, S.W. Hasinoff, and J. Kautz. "Local laplacian filters: Edge-aware image processing with a laplacian pyramid." ACM Trans. Graph. 30.4 (2011): 68.
8. N. Otsu, “A threshold selection method from gray-level histograms”, (1979) IEEE transactions on systems, man, and cybernetics, 9(1), 62-66.
9. R. Achanta et al. "SLIC superpixels compared to state-of-the-art superpixel methods." IEEE transactions on pattern analysis and machine intelligence 34.11 (2012): 2274-2282.
10. M-H. Chen, and P-F. Yan. "A multiscanning approach based on morphological filtering." IEEE Transactions on Pattern Analysis and Machine Intelligence 11.7 (1989): 694-700.
11. J.A. Sethian, J. A. "Level Set Methods and Fast Marching Methods: Evolving Interfaces in Computational Geometry, Fluid Mechanics, Computer Vision, and Materials Science", Cambridge University Press, 1999.
12. H.K Yuen, J. Princen, J. Illingworth, and J. Kittler. "Comparative study of Hough transform methods for circle finding." Image and Vision Computing. Volume 8, Number 1, 1990, pp. 71–77.
13. K. Briechle, and U.D. Hanebeck. "Template matching using fast normalized cross correlation." Optical Pattern Recognition XII. Vol. 4387. International Society for Optics and Photonics, 2001.